JOURNAL OF MATERIALS SCIENCE **34** (1999) 2793–2800

The impact behavior of aluminum alloy 6061: Effects of notch severity

T. S. SRIVATSAN, J. CHAMPLIN, P. C. LAM
Department of Mechanical Engineering, The University of Akron, Akron, Ohio 44325-3903, USA
E-mail: TSrivatsan@UAkron.edu

M. MANOHARAN
Division of Materials Engineering, School of Applied Sciences, Nanyang Technological University, Nanyang Avenue, Singapore 639798

In this paper the influence of notch acuity and test temperature on the impact behavior of aluminum alloy 6061 is presented and discussed. Notch angles of 45°, 60°, 75° and 90° were chosen for a standard charpy impact test specimen containing two such notches positioned at right angles to the applied load. For a given angle of the notch the dynamic fracture toughness increased with an increase in test temperature. At a given test temperature, the impact toughness of a ductile microstructure decreased with an increase in notch severity. For the least severe notch dynamic fracture surfaces revealed the occurrence of localized mixed-mode deformation at the elevated temperature. An increase in notch severity resulted in essentially Mode-I dominated fracture at all test temperatures. The results are discussed in light of alloy microstructure, fracture mechanisms and deformation field ahead of the advancing crack tip.

1. Introduction

Research and development efforts in the field of experimental fracture mechanics, since the early 1950s, have resulted in the emergence and use of many parameters to effectively predict the instability condition in a wide spectrum of mechanical engineering components and civil structures under the influence of a static load. The parameters have also facilitated the characterization of factors and mechanisms governing the static fracture behavior of materials spanning the monolithic metals, the family of intermetallics and their composite counterparts. During this time period the preponderance of scholarly research efforts have been confined to investigating and understanding both material and structural response under essentially Mode I (tension) static loading condition. However, in many practical situations structures are often subjected to a mixed-mode loading and fracture is promoted under dynamic conditions. This has necessitated the need to understand the fracture behavior of materials when subjected to dynamic loads. Classical experimental fracture mechanics approaches to quantifying the energy absorption capability of structures and establishing the mechanisms governing the fracture behavior of materials subjected to dynamic loads has relied to a large extent on impact testing using the Charpy V-notch (henceforth referred to as 'CVN') test specimen. In practical situations it is often possible to have more than one dominant crack in the material that is subjected to dynamic loading. Consequently, establishing the impact toughness and characterizing the fracture behavior of materials having multiple cracks, that is: more than one dominant macroscopic crack, is important in the evolution of appropriate design criteria for structural reliability under conditions of dynamic (impact) loading.

Since the development and standardization of experimental fracture testing techniques for materials and structures, the research efforts of several investigators, during the time period starting the early 1970s, have essentially focussed on characterizing the static fracture toughness of monolithic metals, intermetallics and even their composite counterparts using a compact tension (CT) specimen subjected to: (a) pure Mode I static loading [1–10]; (b) mixed Mode I/Mode III static loading [11–25], and (iii) Mode I/Mode II static loading [26–35]. The imposition of a Mode II loading or Mode III loading on a Mode I load was found to result in a drastic reduction in the static fracture toughness of some materials, whereas in a few others it had only a marginal degradation of the total fracture toughness, an influence dictated by alloy composition and resultant microstructure of the material [36].

The primary objectives of this study were to quantify the energy absorption capability and examine the fracture susceptibility of a material having multiple cracks, of varying degree of severity, and subjected to impact testing using a CVN test specimen.

2. Material and experimental procedures

The material chosen for this study was commercially available aluminum alloy 6061-T651. The as-received

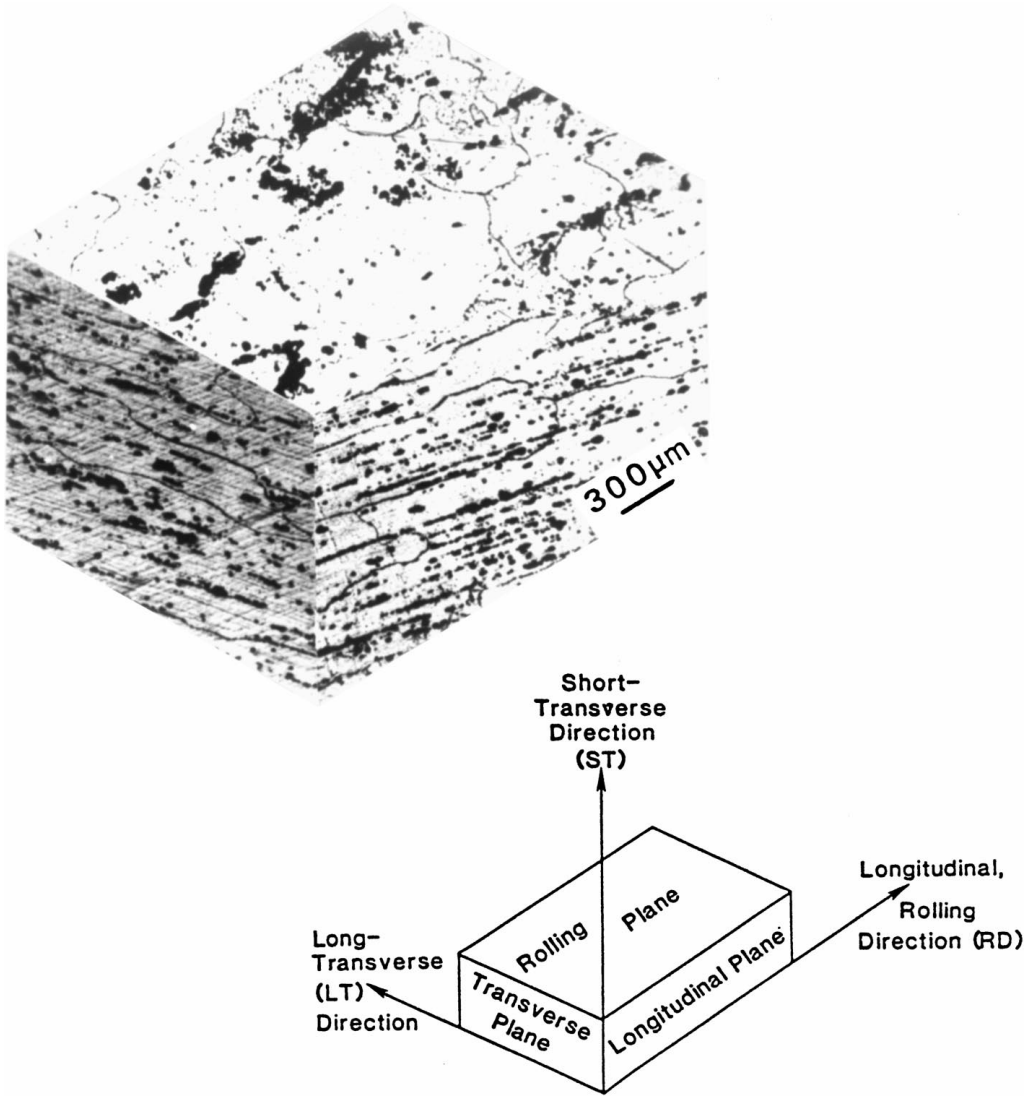

Figure 1 Triplanar optical micrograph illustrating the grain structure of aluminum alloy 6061-T651 along the three orthogonal directions.

TABLE I Nominal chemical composition of aluminum alloy 6061 (in wt %)

Si	Fe	Cu	Mn	Mg	Cr[a]	Al
0.60	0.70	0.30	0.28	1.00	0.20	Remainder

[a] Present as grain refining element.

material is fully recrystallized with fairly large recrystallized grains that were flattened and elongated in the direction of mechanical deformation (rolling) (Fig. 1). The nominal chemical composition of the alloy is given in Table I. The presence of iron as an impurity element in the alloy results in the precipitation of a high volume fraction of coarse iron-rich and even silicon-rich constituents during conventional casting. These particles have been identified to be the compounds Al_7Cu_2Fe and $Al_{12}(FeMn)_3Si$ [37, 38] and range in size from about 3 to 10 μm. The presence of chromium as the grain refining element results in the precipitation of the dispersoids ($Al_{12}Mg_2Cr$) during ingot pre-heat and high temperature homogenization treatments. The chromium dispersoids aid in retaining the directional grain structure developed during mechanical deformation (rolling) of the wrought plate and also assist in preventing the excessive growth of recrystallized grains which form during subsequent heat treatments. The coarse constituent particles and the insoluble magnesium-rich phase (Al_2CuMg) were stratified and distributed along the longitudinal direction (rolling) of the wrought plate. The particles were also found decorating the high-angle grain boundaries (Fig. 2). Silicon and magnesium are present in balance to form the quasi-binary Al-Mg_2Si. The precipitation sequence for this age-hardenable aluminum alloy is: supersaturated solid solution $\rightarrow \beta' \rightarrow \beta(Mg_2Si)$. The Guinier-Preston (G.P.) zones are needle-shaped and form along the $\langle 100 \rangle$ direction of the aluminum matrix [38]. The transition phase β' is rod shaped, has a hexagonal crystal structure and lies along the $\langle 100 \rangle$ direction of the aluminum matrix. The equilibrium precipitate β is face-centered cubic and has a CaF_2 structure, and forms as platelets on the matrix {100} planes [38]. Strengthening in the alloy arises from the presence of the magnesium silicide phase (Mg_2Si), which is the primary hardening precipitate formed during artificial aging of the alloy at temperatures ranging from 433–463 K. A ratio of magnesium to available silicon of 1.7 : 1 ensures that all of the solute is contained in the Mg_2Si phase [38]. The excess silicon in the alloy,

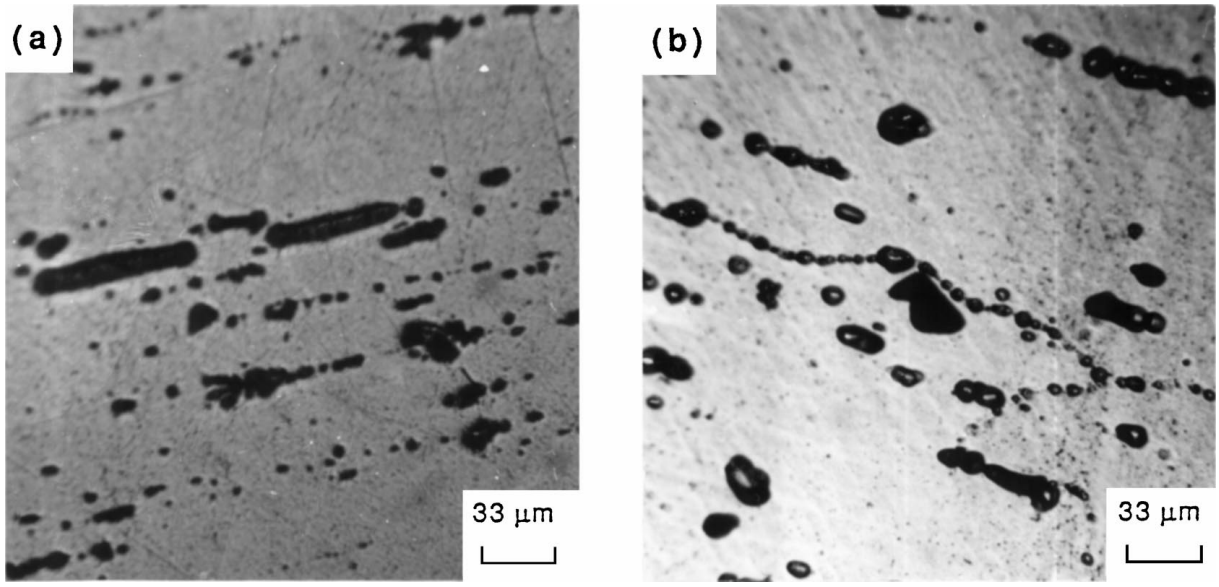

Figure 2 Optical micrographs showing the distribution of coarse constituents in the microstructure.

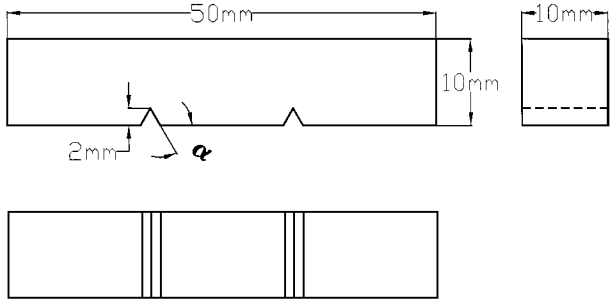

Figure 3 Schematic of the modified Charpy impact test specimen.

TABLE II Influence of temperature on impact toughness of aluminum alloy 6061-T651

Notch angle (degrees)	Energy absorbed (Nm)			
	−190 °C	−70 °C	30 °C	100 °C
45	24	36	37	30
60	18	26	27	42
75	16	27	28	45
90	16	18	19	38

Values are the mean based on duplicate tests.

over and above the amount required for the formation of the ordered Mg_2Si phase, is deposited at the grain boundaries as elemental silicon.

A schematic of the modified CVN test specimen used in this study is shown in Fig. 3. The impact test specimens were prepared from the 6061-T651 rolled plate in the 'TL' orientation. Crack severity was altered by using different angles for the notch. Four notch angles (α: defined in this paper as the inclination of the notch face to the flat surface of the test specimen) of 45°, 60°, 75°, and 90° were chosen for this study (Fig. 3). For a given notch angle the orientation of the two cracks in the test specimen was such that they are parallel to each other and at right angles to the applied load. This modified Charpy impact test specimen provides for a simple method to determine the conjoint and mutually interactive influences of notch severity, impact loading and test temperature on dynamic toughness and fracture resistance of a structure having multiple cracks. Besides providing useful information on the influence of notch severity on impact toughness properties and dynamic fracture characteristics, this study also provides information on the fracture susceptibility of materials having more than one crack. It is hoped that the test concept could be used to rationalize the energy absorbing capability (toughness) and fracture susceptibility of materials having multiple macroscopic flaws of varying severity. This is essential in high volume production industrial settings were the Charpy impact tests are routinely used for purposes of quality control and analysis.

3. Results and discussion

Duplicate tests were performed at temperatures of: (a) liquid nitrogen (−190 °C), (b) dry-ice (−70 °C), (c) ambient (30 °C), and (d) boiling water (100 °C), in accordance with recommended practice [39]. The impact test results are summarized in Table II. For a given notch angle, that is: 45°, 60°, 75°, and 90° (equivalent to a fine slit), the energy absorbed to fracture increased with an increase in test temperature from test temperature of −190 to 100 °C. The overall influence of notch severity and temperature on absorbed energy is exemplified in Fig. 4. Essentially for aluminum alloy 6061 in the peak-aged maximum strength condition (T651), for a given test temperature, the energy absorbed to failure increases with a decrease in notch severity or acuity, that is: angle (α) of the notch. This suggests that increasing the notch severity or acuity is detrimental to dynamic fracture toughness of the alloy for the case of two macroscopic cracks.

The scanning electron micrographs shown in Figs 6–9 support the observations made from measurement of energy absorbed during impact as a function

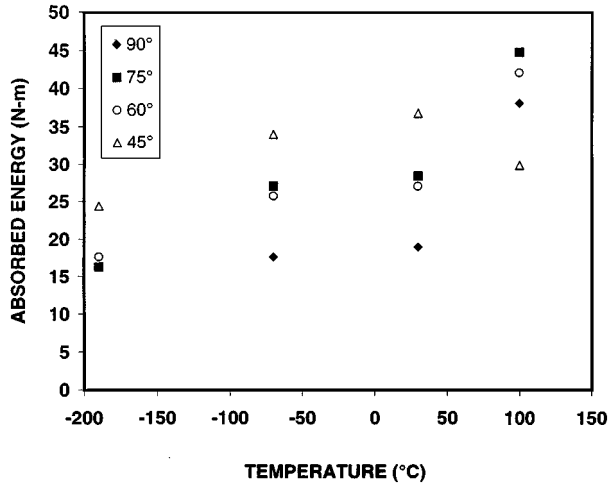

Figure 4 Schematic showing the variation of absorbed energy with test temperature for different degrees of notch acuity.

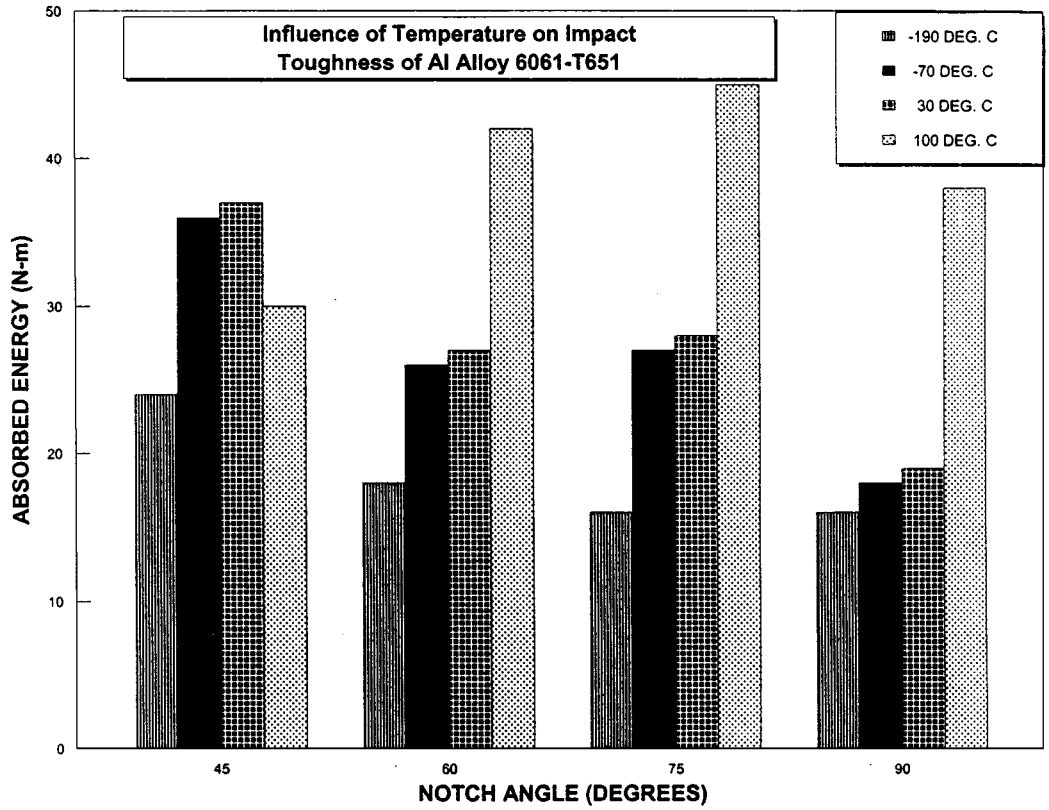

Figure 5 Influence of notch angle and test temperature on absorbed energy (N-m).

of temperature. For notch angle of 45° the fracture surface of the sample deformed at −190 °C revealed the following features:

(a) Cracked particles and numerous microscopic cracks; features reminiscent of locally brittle failure (Fig. 6a).

(b) Ductile tear ridges and isolated pockets of shallow dimples reminiscent of locally ductile failure (Fig. 6b).

At the elevated temperature (100 °C) the impact fracture surfaces revealed evidence of localized shearing as evident through elongated dimples and tear ridges, a population of voids of varying size distributed randomly through the fracture surface, and pockets of shallow equiaxed dimples (Fig. 6c). The occurrence of shear localization ahead of an advancing crack produces incompatibility stresses at interfaces of the second-phase particles in the microstructure, primarily the coarse iron-rich and silicon-rich intermetallics and the insoluble magnesium-rich phase (Al_2CuMg), in the path of the advancing crack causing either fracture of the particle or decohesion at their interfaces, resulting in the formation of microscopic voids. The voids, once formed, tend to exacerbate the localization of shear [40–42] and concurrently limit the size of the plastically deformed region ahead of the advancing crack that is strongly influenced by the Mode I loading component. The net result is the occurrence of highly localized mixed mode

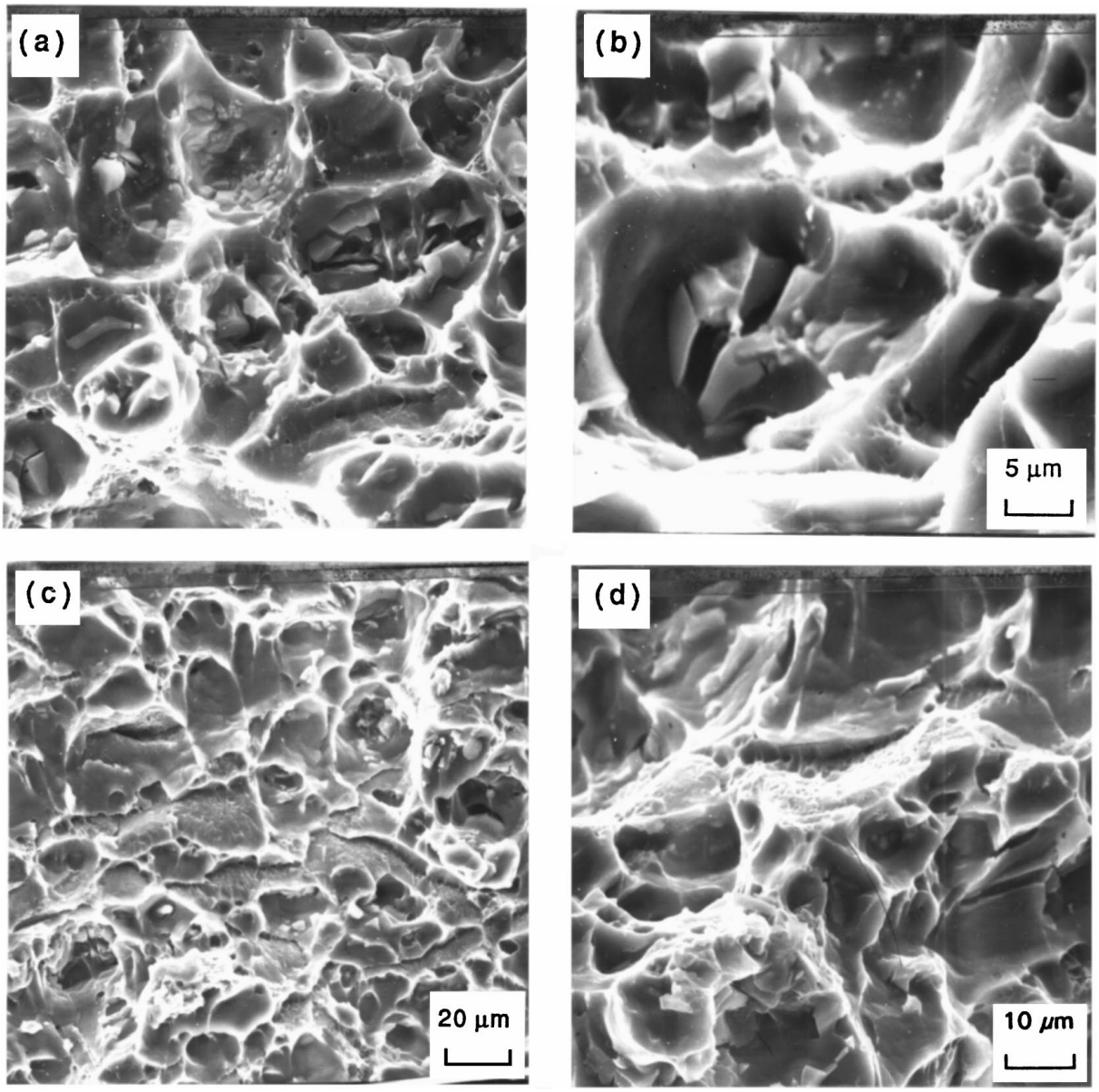

Figure 6 Scanning electron micrographs of the alloy sample with 45° notch and deformed at −190 °C [(a) and (b)] and 100 °C [(c) and (d)], showing: (a) overall morphology of impact fracture surface at −190 °C; (b) cracked particles and shallow equiaxed dimples; (c) elongated dimples, evidence of shearing and macroscopic voids; (d) high magnification of (c).

I/II crack. The presence of a localized Mode II deformation field tends to minimize the Mode I deformation field because of damage associated with localization of shear and causes an apparent reduction in the total fracture toughness. The primary voids are the end result of the early rupture of the brittle intermetallic particles. However, on account of the dynamic nature of loading and the resultant rapid propagation of the crack through the alloy microstructure the fracture process is less governed by either the growth and coalescence of the primary voids or linkage of these voids by the fine secondary void sheets formed around the intermediate size chromium $Al_{12}Mg_2Cr$ dispersoids.

With an increase in notch angle (α) to 60° fracture of the sample dynamically loaded at the cryogenic temperatures [−190 °C and −70 °C] revealed essentially Mode I-dominated failure with the fracture surface comprising: (i) a population of randomly distributed voids of varying size and shape, (ii) tear ridges, (iii) microscopic cracking (Fig. 7a), and (iv) no evidence of either localized shear or elongated dimples in the ductile tear regions (Fig. 7b). The fracture surfaces of the alloy sample dynamically loaded at the ambient (30 °C) and elevated temperatures (100 °C) revealed distinct regions of Mode I dominated failure and isolated pockets of shear (Fig. 7c) suggesting the presence of localized Mode II deformation field at the higher test temperatures. The fracture surfaces were covered with a population of macroscopic voids and ductile tear ridges (Fig. 7d). Pockets of secondary voids were evident along the high-angle grain boundaries. The dimples adjacent to the grain boundaries were shallow suggesting the occurrence of ductile intergranular failure.

Dynamic fracture of the sample with notch angle of 75° was essentially the same at all test temperatures. Fig. 8 shows the fracture features of the sample deformed at room temperature (30 °C). Overall, failure of this ductile microstructure (T651) was Mode I dominated with the fracture surface comprising features reminiscent of locally brittle and ductile failure.

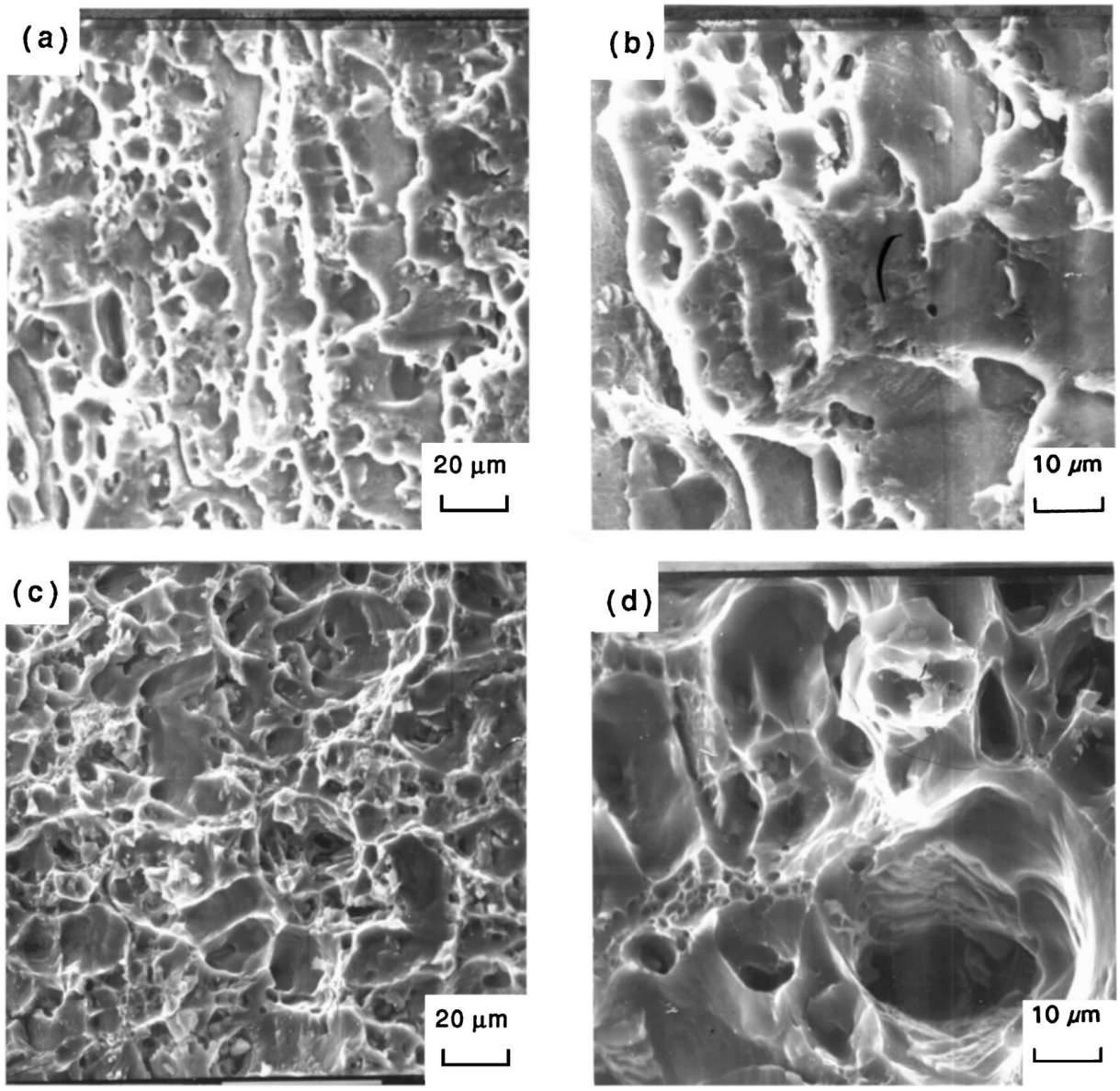

Figure 7 Scanning electron micrographs of fracture surface of dynamically deformed sample with 60° notch showing: (a) voids and microcracking at −70 °C; (b) high magnification of (a); (c) microscopic cracks, population of voids and evidence of local shear; (d) high magnification of (c) showing pockets of dimples along the grain boundaries.

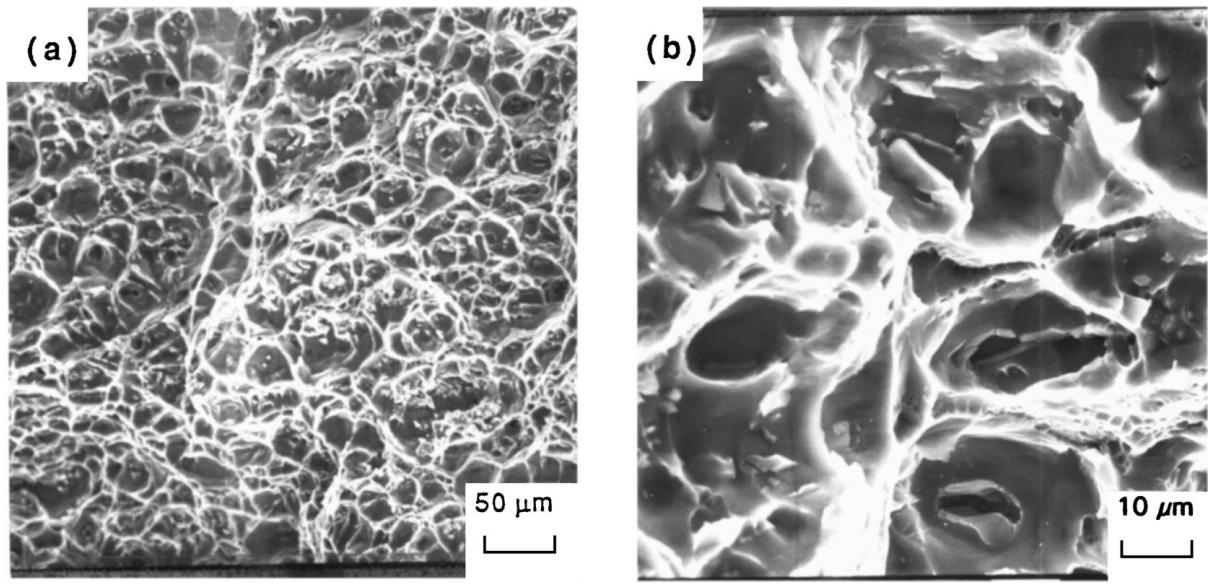

Figure 8 Scanning electron micrographs of sample with notch angle of 75° and dynamically deformed at ambient temperature (30 °C) showing: (a) Overall morphology showing no evidence of localized shear; (b) High magnification of (a) showing voids, cracks and isolated pockets of dimples.

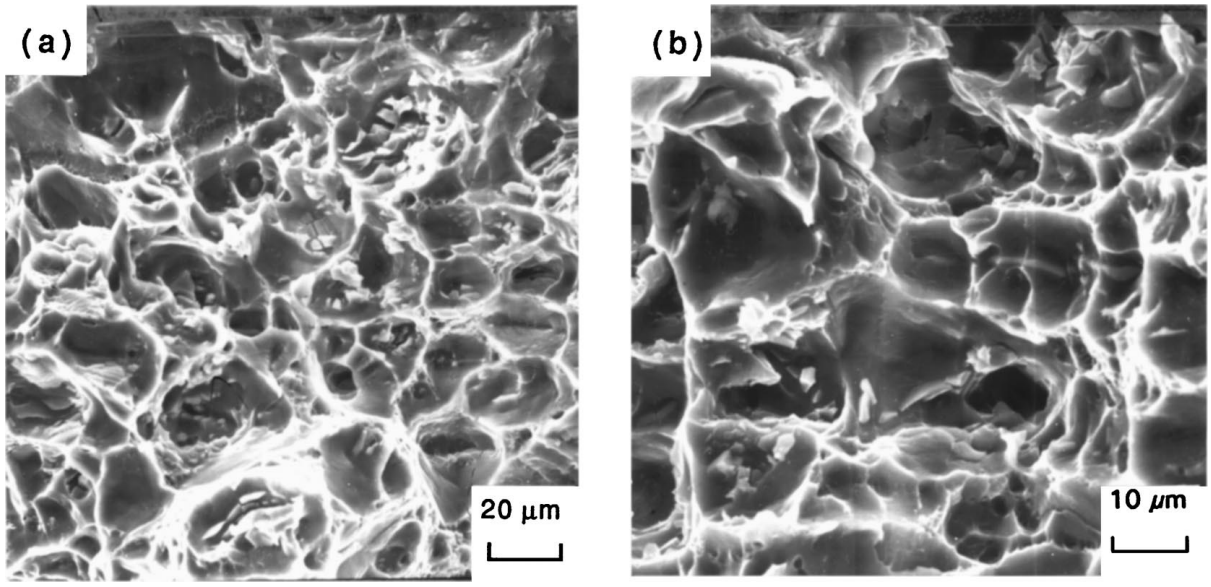

Figure 9 Scanning electron micrographs of sample with notch angle of 90° and deformed dynamically at room temperature (30 °C) showing: (a) Mode I dominated brittle failure with no evidence of shearing; (b) High magnification of (a) showing features reminiscent of locally brittle and ductile mechanisms.

The sample with notch angle of 90° revealed Mode-I dominated failure at all test temperatures with the fracture surface comprising: (i) a large population of microscopic and macroscopic cracks, (ii) tear ridges, and (iii) cracked particles, features reminiscent of locally brittle failure (Fig. 8).

Observation of the fracture surfaces of the alloy samples having two macroscopic cracks and a 45° notch essentially revealed an increase in the dynamic Mode-I fracture toughness with an increase in test temperature resulting in enhanced susceptibility to localized mixed-mode fracture. For this ductile microstructure (T651) of aluminum alloy 6061 the occurrence of localized mixed-mode loading enhances shear localization in the deformation field immediately ahead of an advancing crack tip. This tends to reduce the overall fracture toughness as is evident at the highest test temperature (100 °C) the CVN samples were dynamically deformed.

Increasing the notch angle to 60° resulted in Mode I dominated fracture at the cryogenic temperatures and limited evidence of localized Mode II at the highest test temperature (100°). Further increasing the notch acuity to 75° and 90°, resulted in essentially Mode-I dominated failure at all test temperatures. The occurrence of failure by unstable crack propagation through the alloy microstructure severely restricts the ability of localized shear at limiting the Mode I flow field. Overall failure of the ductile microstructure having multiple macroscopic cracks is essentially brittle, regardless of test temperature. For such conditions of notch acuity (notch angles: 60°, 75°, and 90°) the microstructure has low Mode I dynamic toughness, the influence of any Mode II component on Mode I is at best minimal.

4. Conclusions

Based on a study of the influence of notch severity on the dynamic response and fracture behavior of aluminum alloy 6061 having two macroscopic cracks, the following are the key observations:

1. The current set of experiments using a modified Charpy V-Notch (CVN) specimen suggest that for the very ductile temper of alloy 6061 and for a given notch geometry the dynamic fracture toughness increases with an increase in test temperature.
2. At a given test temperature the notch toughness of alloy 6061-T651 decreases with an increase in notch severity.
3. For the least severe of the notches, i.e., notch angle of 45°, fracture surface appearance suggests the occurrence of localized mixed-mode loading at the elevated temperature enhances the localization of shear in the deformation field immediately ahead of an advancing crack with a concomitant reduction in the overall dynamic fracture toughness of the alloy.
4. With an increase in notch severity or acuity fracture surface appearance reveals essentially Mode I dominated failure at all temperatures with features reminiscent of locally brittle failure.

Acknowledgement

Research supported by The University of Akron (Akron, Ohio, USA) and The State of Ohio: Board of Regents (Columbus, Ohio, USA).

References

1. J. G. KAUFMAN, Developments in fracture mechanics test methods, STP 632, American Society for Testing and Materials, Philadelphia, USA, 1977, pp. 3–24.
2. National Materials Advisory Board Report, NMAB-328, 1976, N-78-72695.
3. F. G. NELSON and J. G. KAUFMAN, Fracture toughness testing at cryogenic temperatures, STP 496, American Society for Testing and Materials, Philadelphia, USA, 1971, pp. 27–39.
4. D. O. SPROWLS, M. B. SHUMAKER, J. D. WALSH and J. W. LARSEN, NASA-CR-124469: Part I, National Aeronautics and Space Administration, USA, 1973.

5. J. P. GUDAS and J. A. JOYCE, David Taylor Ship Research and Development Center Report 781054, 1978.
6. G. SUCCOP, R. T. BUBSEY, M. H. JONES and W. F. BROWN, Jr., Developments in fracture mechanics test methods standardization, STP 632, American Society for Testing and Materials, Philadelphia, USA, 1977, pp. 153–178.
7. J. L. SHANNON, JR., J. K. DONALD and W. F. BROWN, Jr., Developments in fracture mechanics test methods standardization, STP 632, American Society for Testing and Materials, 1977, pp. 96–114.
8. F. G. NELSON and D. J. BROWN, Flaw growth and fracture, STP 631, American Society for Testing and Materials, Philadelphia, PA, USA, 1977, pp. 285–309.
9. T. D. MOORE (ed.) "Structural Alloys Handbook, Battelle Columbus Laboratories," 2nd ed. (1978).
10. P. C. PARIS, H. TADA, A. ZAHOOR and H. ERNST, Elastic-plastic fracture, STP 668, American Society for Testing and Materials, Philadelphia, PA, USA, pp. 5–36.
11. M. YODA, *Engineering Fracture Mechanics* **13** (1980) 647.
12. Y. UEDA, K. IKEDA, T. YAO and M. AOKI, *ibid.* **18** (1983) 1131.
13. M. T. MIGLIN, I. H. LIN, J. P. HIRTH and A. R. ROSENFIELD, ASTM STP 791, American Society for Testing Materials, 1983, p. 353.
14. M. T. MIGLIN, J. P. HIRTH and A. R. ROSENFIELD, *International Journal of Fracture* **22** (1983) R65.
15. *Idem., Res. Mechanica* **11** (1984) 85.
16. Z. H. LIU and W. SHEN, *International Journal of Fracture* **25** (1984) R. 21.
17. J. G. SCHROTH, J. P. HIRTH, R. G. HOAGLAND and A. R. ROSENFIELD, *Metallurgical Transactions* **18A** (1987) 1061.
18. M. MANOHARAN, J. P. HIRTH and A. R. ROSENFIELD, *Scripta Metall.* **23** (1989) 763.
19. S. V. KAMAT, J. P. HIRTH and R. MEHRABIAN, *ibid.* **23** (1989) 523.
20. M. MANOHARAN, S. RAGHAVACHARY, J. P. HIRTH and A. R. ROSENFIELD, *Journal of Engineering Materials Technology* **111** (1989) 440.
21. S. RAGHAVACHARY, A. R. ROSENFIELD and J. P. HIRTH, *Metallurgical Transactions* **21A** (1990) 2539.
22. M. MANOHARAN, J. P. HIRTH and A. R. ROSENFIELD, *Journal of Testing and Evaluation* **18** (1990) 106.
23. *Idem., Acta Metall. Materialia* **39** (1991) 1203.
24. A. M. KUMAR and J. P. HIRTH, *Scripta Metall. Materialia* **25** (1991) 981.
25. A. M. KUMAR, S. V. KAMAT and J. P. HIRTH, in Proceedings of Morris E. Fine Symposium, edited by P. K. Liaw, J. R. Weertman, H. L. Marcus and J. S. Santner (The Minerals, Metals and Materials Society, Warrendale, PA, 1991) p. 313.
26. T. M. MACCAGNO and J. F. KNOTT, *Engineering Fracture Mechanics* **34** (1989) 65.
27. D. K. MAHANTY and S. K. MIATI, *ibid.* **37** (1990) 1237.
28. S. AOKI, K. KISHIMOTO, T. YOSHIDA, M. SAKADA and H. A. RICHARD, *Journal of Mechanics and Physics Solids* **38** (1990) 195.
29. A. M. A. MAGEED and R. K. PANDEY, *Engineering Fracture Mechanics* **40** (1991) 371.
30. T. M. MACCAGNO and J. F. KNOTT, *ibid.* **38** (1991) 111.
31. *Idem., ibid.* **41** (1992) 805.
32. K. TOHGO and H. ISHII, *ibid.* **41** (1992) 529.
33. J. A. WALSH, K. V. JATA and E. A. STARKE, JR., *Acta Metall. Materialia* **37** (1989) 2861.
34. D. BHATTACHARJEE and J. F. KNOTT, *ibid.* **42** (1994) 1747.
35. M. MANOHARAN, *J. Mater. Sci. Letts.* **15** (1996) 254.
36. X. FENG, A. M. KUMAR and J. P. HIRTH, *Acta Metallurgica Materialia* **41** (1993) 2755–2765.
37. E. A. STARKE, JR., *Materials Science and Engineering* **29** (1977) 99–115.
38. E. A. STARKE, JR., in "Treatise in Materials Science and Technology," Vol. 31, edited by A. K. Vasudevan and R. D. Doherty (Academic Press, 1989) p. 35.
39. ASTM Standards E-23-93, Standard method for notched bar impact testing of metallic materials (American Society for Testing Materials, Philadelphia, PA, USA).
40. V. TVERGAARD, *Journal of Mechanics and Physics of Solids* **35** (1987) 43.
41. N. A. FLECK and J. W. HUTCHINSON, in Proceedings Royal Society of London A, 1986, Vol. 407, p. 435.
42. S. V. KAMAT and J. P. HIRTH, *Acta Materialia* **44** (1996) 201.
43. M. MANOHARAN, *Scripta Materialia* **35**(8) (1996) 933–937.

Received 30 July 1998
and accepted 13 January 1999